FINITE ELEMENT MODELING OF THE HYGROSCOPIC WARPING OF MEDIUM DENSITY FIBERBOARD

Stefan Ganev

Former Ph.D. candidate
Groupe interdisciplinaire de recherche en éléments finis (GIREF)
Département des sciences du bois et de la forêt
Université Laval
Québec, Canada G1K 7P4
and Senior Composite Scientist
Forintek Canada Corp.
319, rue Franquet
Sainte-Foy, Québec, Canada G1P 4R4

Alain Cloutier†

Professor
Groupe interdisciplinaire de recherche en éléments finis (GIREF)
Département des sciences du bois et de la forêt
Université Laval
Québec, Canada G1K 7P4

Guy Gendron

Professor
Groupe interdisciplinaire de recherche en éléments finis (GIREF)
Département de génie mécanique
Université Laval
Québec, Canada, G1K 7P4

and

Robert Beauregard†

Associate Professor
Département des sciences du bois et de la forêt
Université Laval
Québec, Canada G1K 7P4

ABSTRACT

The objective of this study was to develop a three-dimensional finite element model of the hygrome-chanical deformation of medium density fiberboard (MDF) panels with various vertical density profiles subjected to moisture adsorption on one face. The theoretical model was based on three sets of equations: 1) three-dimensional equations of unsteady-state moisture diffusion, 2) three-dimensional equations of mechanical equilibrium, and 3) Hooke's law for plane isotropy, which takes into account shrinkage and swelling through the panel thickness. The finite element model was applied to six panels with various density profiles. For both the simulations and the experiments, the warping was caused by moisture adsorption from one of the faces of 560-mm × 560-mm × 12-mm MDF panels while the other surface and the edges were sealed. Physical and mechanical characteristics defined as a function of density and moisture content were used as model inputs. The model made it possible to capture the rapid initial development of maxi-

---

† Member SWST.

mum warp and its following decrease as moisture content equalized through panel thickness; the effect of the density profile on the level of warp caused by moisture adsorption; and warp fluctuations resulting from changes in the ambient relative humidity, and from the hysteresis in the expansion coefficient between adsorption and desorption. To validate the model, the warp development of laboratory MDF panels was compared to simulation results. The agreement between calculated and actual panel warping confirmed that the model could successfully be used to simulate moisture movement in MDF and the resulting warp, and to help in the optimization of panel vertical density profiles aiming at better stability of form in MDF panels. For the typical experimental cases, it was observed that there was a strong effect of panel density profile on the levels of warp and its dynamics. The levels of warp increased with average panel density. The panels with sharper density profile developed stronger warp compared to panels with an even profile. When the density profile was skewed towards one of the surfaces, the panel developed positive or negative warp and did not return to the original flat form.

Keywords: MDF (medium density fiberboard), hygromechanical warping, finite element model, elastic properties, density profile, moisture diffusion.

INTRODUCTION

Medium density fiberboard (MDF) panels are expected to maintain stability of form, since they are used in furniture, cabinetry, and other high-value applications. For cost-effectiveness or appearance purposes, there is a trend in the industry to overlay cabinetry elements (e.g. kitchen cabinet doors) from one side only or to apply different overlays on both panel sides. As a result, an asymmetrical moisture-content-profile (M-profile) develops across panel thickness when the ambient RH changes causing deviations from panel initial flatness, or warp (Suchsland and McNatt 1986). Depending on its level, warp can hinder further processing such as vacuum handling, machining, and assembling, or it can affect the performance of final products such as furniture, flooring, or cabinetry with the result that panels have to be recycled or discarded. The further along the value-adding chain the problems occur, the greater the financial losses.

With its characteristic density profile through the thickness, MDF can be represented as a layered composite with each layer at a particular density level. In such a structure, tensile and shear moduli, shrinkage and swelling, and diffusion coefficients in the three principal panel directions are specific for each density layer. Furthermore, when moisture content (M) is unevenly distributed through MDF panel thickness, layer properties such as dimensions, moduli, of elasticity, shear moduli, and Poisson's ratios vary accordingly. For example, linear expansion increases,

while modulus of elasticity decreases. The effects of the density profile and M-profile on MDF stability of form have not been systematically studied. Theoretical modeling based on knowledge of the governing equations (models) and their solutions with the finite element method (FEM) allows the simulation of the water vapor movement in MDF and the corresponding deformation. Simulations for various panel structures can help optimize the design of wood composite panels.

Objective

The objective of this paper is to present a three-dimensional finite element model of the hygromechanical deformation and its application to the study of MDF panels with various density profiles exposed to moisture adsorption from one surface at constant ambient temperature.

BACKGROUND

Warp has been defined as the deviation of the geometry of a panel from an initial form of flatness (Suchsland and McNatt 1985). Depending on the location of measurement and shape of the deformed specimen, warp is differentiated as: "cup," a deformation along the width, "bow," a deformation along the length and "twist," a deviation from a flat plane between diagonal corners (NPA 1996). In some cases, a more complex, saddle-shaped deformation can be observed

(Suchsland et al. 1995). Our experiments showed that in MDF panels without specific machine direction, e.g. hand-formed laboratory specimens, cup and bow are equal in size and are always oriented toward the same side. An example of a panel with convex deformation towards the exposed (bottom) side is given in Fig. 1. Consequently, in such panels there are no conditions for saddle-shaped form, which could appear if one panel edge becomes concave, while the perpendicular edge becomes convex. The level of warp is a function of the span over which it is measured (Norris, in Heebink et al. 1964). Since the diagonal presents the longest panel dimension, the deviation from flatness is the largest along the diagonal cross-section of the panel (at the center of the surface). Therefore, in this study, the deviation from the ideal flat form at cross-section of diagonals has been adopted as a measure of warp.

Usually, it is an asymmetrical strain distribution throughout panel thickness that causes warp. Often, dissymmetry with respect to panel mid-plane of the moisture content profile and material properties causes the strain differential (Suchsland et al. 1995). Given the large surface to edge ratio in typical MDF specimens, moisture movement parallel to the surface is much smaller and thus negligible. The temperature gradient could have a similar effect. However, the effect of one-percent M-change on wood dimensions is about twenty times greater than the effect of a temperature change of one-degree Kelvin (Forest Products Laboratory 1987). Therefore, our study concentrates on the effect of moisture movement on warp.
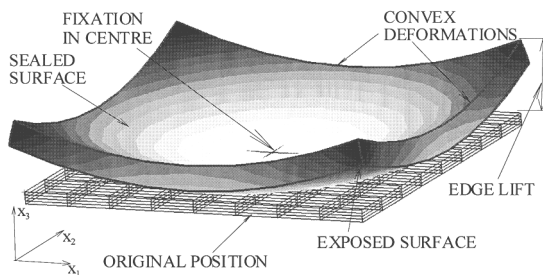

Fig. 1.   Convex deformation in a FE model.

As a rule, medium density fiberboard is homogeneous across thickness in terms of fiber geometry and resin content (CPA 1998). The main variability is the density profile, a result of the uneven densification due to a temperature and moisture content differential across thickness during pressing. There is a strong effect of MDF density on thickness swell (Suchsland 1973; Vital and Wilson 1979; Winistorfer and Xu 1996), linear expansion (Woodson 1975; Ganev and Cloutier 2002), moisture adsorption (Denisov et al. 1975; Schneider et al. 1982; Bolton and Humphrey 1994; Vital and Wilson 1979), and moduli of elasticity (e.g. Plath 1972). Consequently, average panel density and density profile are the dominant properties determining panel stability of form. Similar to particleboard, in MDF the zones in the density profile through the thickness that are characterized by specific density can with approximation be considered as discrete layers. The closer the layers to the panel surface, the higher their density. In addition, depending on their distance from the central plane, different layers have different impact on the overall panel performance. It has been demonstrated, for example, that for a typical three-layer particleboard only one-third of the bending moment is supported by the core layer, with two-thirds supported by the surface layers, which occupy only 40 % of the overall panel thickness (Keylwerth 1958). As a result, at equal average density, it could be expected that the sharper the density profile, the stronger the effect of the surface layer on the overall panel properties, including stability.

The effect of the layer characteristics on warp has been outlined in several theoretical models. Norris (in Heebink et al. 1964) proposed a two-dimensional solution of Hooke's law as a model of warp for panels subject to M-change. This solution expresses warp at a specific point in time as a function of the mechanical and expansion characteristics of each panel layer at any selected moment of time. The model is not suitable for simulating the dynamics of warp development following ambient humidity changes because it allows only for discrete solutions valid at a given point in time, at which all panel properties are

known. It does not take into consideration the effect of moisture penetration on the thickness swell of the layers or on their linear expansion in two perpendicular directions in the panel plane. The model of Norris (in Heebink et al. 1964) was later applied by Suchsland and McNatt (1986) for simulation of the warping of plywood and by Suchsland et al. (1995) for calculating the warp of overlaid particleboard. Ismar and Paulitsch (1995) used a similar approach, considering in addition a thermal effect. As discussed earlier, the effect of temperature is relatively small compared to the effect of moisture. Tong and Suchsland (1993) presented a finite element model of the warp of wood composites based on an elastic constitutive law. In their model, the water vapor movement through panel thickness was not included and no solutions were presented for MDF. We consider that the water vapor movement in the panel should be an integral part of a model of warp. To improve the accuracy of a model of warp in plywood, Xu (1993) developed a model based on a visco-elastic constitutive law because high differences between linear expansion coefficient (LEC) and modulus of elasticity in the x_1 direction (E_1) of consecutive longitudinal and cross-oriented layers through the thickness may lead to inelastic deformations. The authors explained that in composite panels such as MDF the differences in expansion values and moduli of elasticity between consecutive layers are much smaller than those between plywood cross plies. This leads to relatively small lamina strains and swelling stresses in MDF and therefore plastic deformations are not provoked. Related to this, Xu (1994) and Xu and Suchsland (1996) made the observation that for MDF and particleboard an elastic-type of behavior is observed. Lang et al. (1995) also disregarded the visco-elastic effect referring to the temporary character of the M-gradient. The elastic equation they used overestimated warp in plywood and oriented strandboard (OSB) by approximately 15 %. The overestimation was attributed to the natural imperfection of the constituting veneers.

Our preliminary calculations with the FEM showed, that at the warp climax, the highest stresses experienced by the MDF panel did not exceed 25 % of the stress at the proportional limit determined experimentally. Consequently, we considered MDF as an elastic material at the temperature and in the M-ranges considered in this study. Based on the literature (Tong and Suchsland 1993; Xu and Suchsland 1996) and our preliminary trials, a three-dimensional elastic constitutive law and the moisture diffusion equation were adopted for modeling the warp in MDF for this study.

The finite element (FE) method is a potent approach for solving differential equations as those describing the phenomenon of warp. This is the method that we have selected over more traditional approaches.

MATERIAL AND METHODS

Material

Medium density fiberboard panels of dimensions 650 mm x 650 mm x 12 mm were made in the laboratory from softwood fibers produced from green black spruce (*Picea mariana*) chips at three nominal density levels, namely 540 kg/m³, 650 kg/m³, and 800 kg/m³. A urea-formaldehyde binder was used. The components were mixed in a laboratory rotary blender. The 650-mm x 650-mm mats were first pre-pressed and then hot-pressed in a Dieffenbacher press. Each panel was edge-trimmed to 560 mm x 560 mm x 12 mm to discard the weak area next to the edges. As a result, a diagonal length of the flat surface of 792 mm was obtained. The panel surface layers were sanded off, reducing the panel thickness to 10.5 mm, to obtain panels without density profile at the three nominal density levels: 540 kg/m³, 650 kg/m³, and 800 kg/m³, or with the desired density profiles e.g. 540 kg/m³ for the surface layer and 900 kg/m³ as maximum density in the core layer. A more detailed description of the manufacturing of the laboratory panels is given in Ganev et al. (2004a).

Methods

The warping of MDF specimens was induced by allowing moisture adsorption through one of the panel surfaces. During the entire experiment, the temperature was kept constant at 20°C. This allowed excluding temperature as a factor of warp. The specimens were initially conditioned

to 50 % RH. One large face and all panel edges were sealed with a thin silicone layer. A 0.1-mm-thick polyethylene foil was directly applied on the silicone layer. The samples were then exposed to 80 % RH in a conditioning room. This allowed moisture to penetrate from the exposed surface inward in the thickness direction, while moisture diffusion through panel edges was restricted. The MDF specimens were allowed to expand and deform in any direction. The dynamics of warp was monitored by recording the maximum deformation at the center of the exposed surface until equilibrium to 80 % RH was reached. When the deformation was convex towards the exposed surface, the warp was called "positive." In FE simulation with panel center fixed and corners free to move, this translated into panel corners lifting in the positive x_3 direction away from the initial flat form. When the deformation was concave towards the exposed surface, it was called "negative." In FE simulation with panel center fixed and corners free to move, this translated into panel corners dropping in the negative x_3 direction away from the initial flat shape. An example of convex deformation obtained by FE simulation is given in Fig. 1.

Mathematical model

The theoretical model was based on three sets of equations: 1) three-dimensional equations of unsteady-state moisture diffusion, 2) three-dimensional equations of mechanical equilibrium, and 3) Hooke's law for plane isotropy which takes into account the shrinkage and swelling of each layer through panel thickness. The moisture transfer equation can be written in the following way:

$$\frac{\partial M}{\partial t} - \left\{ \frac{\partial}{\partial x_1} \quad \frac{\partial}{\partial x_2} \quad \frac{\partial}{\partial x_3} \right\}$$

$$\left[\begin{pmatrix} D_1 & 0 & 0 \\ 0 & D_2 & 0 \\ 0 & 0 & D_3 \end{pmatrix} \left\{ \begin{array}{c} \dfrac{\partial M}{\partial x_1} \\ \dfrac{\partial M}{\partial x_2} \\ \dfrac{\partial M}{\partial x_3} \end{array} \right\} \right] = 0 \qquad (1)$$

where: M = moisture content (oven-dry basis) (kg kg^{-1} x 100);
   t = time (s)
   D_i = effective diffusion coefficient (m^2 s^{-1}).

The mechanical model is based on the equations of equilibrium:

$$\frac{\partial \sigma_{ij}}{\partial x_i} = 0 \qquad\qquad i, j = 1, 2, 3 \qquad (2)$$

where: σ_{ij}: components of the stress tensor (Pa) and summation is implied on repeated indices.

The components of the stress tensor are calculated using a stress-strain moisture relation for orthotropic material. If the principal material directions coincide with the principal directions of the panel, this relation can be written as follows:

$$\left\{ \begin{array}{c} \sigma_1 \\ \sigma_2 \\ \sigma_3 \\ \sigma_{23} \\ \sigma_{13} \\ \sigma_{12} \end{array} \right\} = \left[\begin{array}{cccccc} \dfrac{1-v_{23}v_{32}}{E_2 E_3 S} & \dfrac{v_{21}+v_{23}v_{31}}{E_2 E_3 S} & \dfrac{v_{31}+v_{21}v_{32}}{E_2 E_3 S} & 0 & 0 & 0 \\[2mm] \dfrac{v_{21}+v_{23}v_{31}}{E_2 E_3 S} & \dfrac{1-v_{31}v_{13}}{E_2 E_3 S} & \dfrac{v_{23}+v_{21}v_{13}}{E_1 E_2 S} & 0 & 0 & 0 \\[2mm] \dfrac{v_{31}+v_{21}v_{32}}{E_2 E_3 S} & \dfrac{v_{23}+v_{21}v_{13}}{E_1 E_2 S} & \dfrac{1-v_{21}v_{12}}{E_1 E_2 S} & 0 & 0 & 0 \\[2mm] 0 & 0 & 0 & G_{23} & 0 & 0 \\ 0 & 0 & 0 & 0 & G_{13} & 0 \\ 0 & 0 & 0 & 0 & 0 & G_{12} \end{array} \right]$$

$$\left(\left\{ \begin{array}{c} \varepsilon_1 \\ \varepsilon_2 \\ \varepsilon_3 \\ \varepsilon_{23} \\ \varepsilon_{13} \\ \varepsilon_{12} \end{array} \right\} - \left\{ \begin{array}{c} \beta_1 \Delta M \\ \beta_2 \Delta M \\ \beta_3 \Delta M \\ 0 \\ 0 \\ 0 \end{array} \right\} \right) \qquad (3)$$

$$\text{with } \ S = \frac{1}{E_1 E_2 E_3}$$

$$\left(1 - 2v_{21}v_{32}v_{13} - v_{13}v_{31} - v_{23}v_{32} - v_{12}v_{21} \right) \qquad (4)$$

where: ε_{ij} = strain components vector;
   β_i = shrinkage/swelling expansion coefficient vector (%$^{-1}$);
   ΔM = moisture content change (%);
   E_i = moduli of elasticity (Pa);
   G_{ij} = shear moduli (Pa);
   v_{ij} = Poisson's ratios.

The strains, ϵ_{ij} are related to displacements, u_i, through the following relation:

$$\varepsilon_{ij} = \tfrac{1}{2}\left(\frac{\partial u_i}{\partial x_j} + \frac{\partial u_j}{\partial x_i}\right)$$
(5)

For isotropic materials, $E_1 = E_2 = E_3 = E$; $G_{23} = G_{13} = G_{12} = G$; $\nu_{12} = \nu_{13} = \nu_{21} = \nu_{23} = \nu_{31} = \nu_{32} = \nu$; and $\beta_1 = \beta_2 = \beta_3 = \beta$; $D_1 = D_2 = D_3 = D$. Medium density fiberboard can be assumed as plane isotropic (Bodig and Jayne 1993). In the case of the current study, $E_1 = E_2$, $G_{23} = G_{13}$, $\nu_{12} = \nu_{21}$, $\nu_{23} = \nu_{32} = \nu_{13} = \nu_{31}$, $\beta_1 = \beta_2$ and $D_1 = D_2$. The shear modulus G_{12} can be obtained from E_1 and ν_{12} as follows:

$$G_{12} = \frac{E_i}{2(1+\nu_{12})}$$
(6)

Because of the insulation of panel edges and the large length to thickness ratio in the panels, it was considered that no significant diffusion occurs in directions parallel to panel plane, or $D_1 = D_2 = 0$. Consequently, eight independent parameters need to be known as a function of density and M for the solution of Eq. (1) and (2): D_3, E_1, E_3, ν_{12}, ν_{13}, and G_{13} as a function of density and M; β_1 and β_3 as a function of density and sorption direction.

Finite element modeling of hygromechanical warping of MDF

The finite element model is based on the Galerkin weak variational formulation of Eqs. (1) and (2). The unsteady-state moisture transfer equation (Eq.1) is solved using a time integration scheme. The steps are automatically selected by ABAQUS, which automatically subdivides a large time step into several smaller increments if it finds that the solution is nonlinear. This process is completely automatic, and ABAQUS always takes the largest possible time increments that will reach the end of the step and still give an accurate, convergent solution. At each time step, the moisture content change (ΔM) is found, and it is used to calculate the corresponding displacements and strains.

The finite element mesh used for modeling the MDF specimen described previously is shown in Fig. 2. In fact, since the problem is symmetrical about x_1 and x_2, only one-fourth of the original panel is modeled and symmetry boundary conditions (BC) are defined. A total of 768 hexahedral 8-node elements are used. The mesh was refined until the change in the model results became smaller than the accuracy of the warp measurement. In analogy with particleboard, each FE model was divided into 2 surface layers (each with thickness 1.4 mm) and one core layer (with

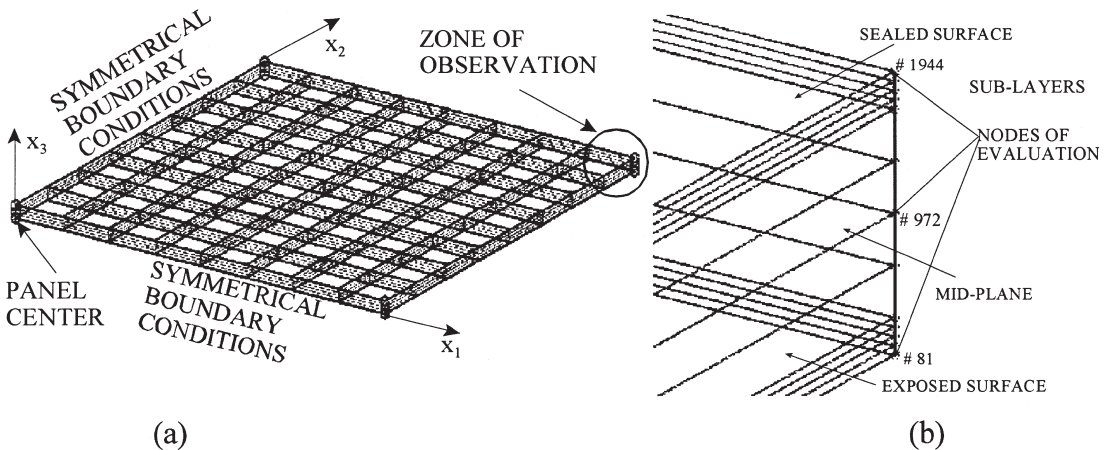(a)   (b)

FIG. 2. Finite element mesh: a) complete mesh (768 hexahedral 8-node elements); b) cross-section of mesh at panel corner (zone of maximum deformation).

thickness 7.7 mm). This reflected the typical density distribution throughout the MDF panel thickness. Four sub-layers, each consisting of one row of elements with a thickness of 0.35 mm represent each of the two surface layers and four sub-layers each consisting of one row of elements with a thickness of 1.925 mm represent the core layer. Each sub-layer can be assigned a different density level, with corresponding mechanical and expansion characteristics as determined in Ganev et al. (2004b). This allows for flexibility in designing various density profiles. Water vapor adsorption by convection was limited to the "exposed" surface only. Each layer of the panel is assumed isotropic in the plane and elastic.

The following initial and boundary conditions were used for Eq. (1):

Initial condition

$$M\left(x_1, x_2, x_3, t_0\right) = M_0 \; \forall\left(x_1, x_2, x_3\right) \qquad (7)$$

Boundary conditions

$$q = h\left(M_s - M_\infty\right) \text{ on exposed surface} \qquad (8)$$

$$q = 0 \text{ on edges and "sealed" surface} \qquad (9)$$

where q: moisture flux
    M_0: initial moisture content of the panel (%);
    M_s: surface moisture content of MDF (%);
    M_∞: moisture content of MDF at equilibrium (%);
    h: convective mass transfer coefficient (kg m^{-2} s^{-1} %$^{-1}$).

For the solution of Eq. (7) to (9), M_s is unknown, while all other quantities are known based on the preliminary experiments (Ganev et al. 2003, 2004a, 2004b). For the convective mass transfer coefficient (h), a value of 0.000032 kg m^{-2} s^{-1} %$^{-1}$ (Cloutier et al. 2001) was obtained by calculation based on a methodology proposed by Siau (1995).

For the FE simulations, M_0 was set at 6.5 % and M_∞ was set at 12.5 %. Even at initial equilib-

rium at 50 % RH, there is vertical M-distribution (M-profile, Xu et al. 1996) due to the impact of density profile on the sorption isotherm (Ganev et al. 2003). However, layers with higher M_0 equilibrate also at higher M_∞ and vice-versa. Therefore the effect of the density profile on the initial M-profile was neglected assuming that this will not significantly affect the results in terms of warping.

The model parameters used are summarized in Table 1. The parameters were calculated for the specific density and M-levels corresponding to the exposures of the specimens for warping. The calculations are based on multiple regression models obtained from experimental results (Ganev et al. 2004a and 2004b). The following initial and boundary conditions were used for the mechanical part of the problem:

Initial conditions

$$\sigma\left(x_1, x_2, x_3, t_0\right) = \sigma_0 = 0 \; \forall\left(x_1, x_2, x_3\right) \quad (10)$$

$$u\left(x_1, x_2, x_3, t_0\right) = u_0 = 0 \; \forall\left(x_1, x_2, x_3\right) \quad (11)$$

Boundary conditions

$$u_1 = 0 \; at\left(0, x_2, x_3\right) \qquad (12)$$

$$u_2 = 0 \; at\left(x_1, 0, x_3\right) \qquad (13)$$

$$u_3 = 0 \; at\left(0, 0, 0\right) \qquad (14)$$

Symmetry boundary conditions

$$u_1 = 0 \; at\left(0, x_1, x_3\right) \qquad (15)$$

$$u_2 = 0 \; at\left(x_1, 0, x_3\right) \qquad (16)$$

The finite element modeling of the hygromechanical warping of MDF was performed using the finite element software ABAQUS and the pre- and post-processing software PATRAN. A user subroutine was written in FORTRAN to take into consideration the hysteresis in the expansion properties between adsorption and desorption. In the case of adsorption, the user subroutine applies specific values of linear expansion and thickness swell coefficients charac-

TABLE 1. *Parameters used in the finite element models.*

Property	Units	Nominal density (kg/m³)							
		540		650		800		900	
		Moisture level (%)							
		6.6	9.0	6.6	9.0	6.6	9.0	6.6	9.0
E_1, E_2	(Pa)	7.4×10^8	6.3×10^8	1.3×10^9	1.1×10^9	2.2×10^9	1.9×10^9	2.8×10^9	2.5×10^9
E_3	(Pa)	1.7×10^7	1.2×10^7	3.5×10^7	2.6×10^7	6.1×10^7	4.4×10^7	7.8×10^7	5.6×10^7
ν_{12}	(–)	0.3	0.3	0.3	0.3	0.3	0.3	0.3	0.3
ν_{13}, ν_{23}	(–)	0.2	0.2	0.2	0.2	0.2	0.2	0.2	0.2
G_{12}	(Pa)	2.8×10^8	2.4×10^8	4.9×10^8	4.5×10^8	8.5×10^8	7.5×10^8	1.1×10^9	9.4×10^8
G_{13}, G_{23}	(Pa)	8.4×10^7	7.1×10^7	1.2×10^8	0.9×10^8	1.3×10^8	1.0×10^8	1.9×10^8	1.4×10^8
D	(m²/s)	1.0×10^{-9}	9.9×10^{-11}	9.3×10^{-10}	8.9×10^{-11}	8.0×10^{-10}	8.0×10^{-11}	7.2×10^{-10}	7.6×10^{-11}
		Adsorption							
$\beta_1, \beta_2,$	(%⁻¹)	1.7×10^{-4}		2.3×10^{-4}		3.6×10^{-4}		3.9×10^{-4}	
β_3	(%⁻¹)	7.4×10^{-3}		7.7×10^{-3}		8.4×10^{-3}		8.7×10^{-3}	
		Desorption							
$\beta_1, \beta_2,$	(%⁻¹)	3.4×10^{-4}		4.8×10^{-4}		7.7×10^{-4}		10.0×10^{-4}	
β_3	(%⁻¹)	5.4×10^{-3}		6.2×10^{-3}		9.5×10^{-3}		1.1×10^{-2}	

teristic for each density level. In the case of desorption, the user subroutine applies corresponding values of linear contraction and thickness shrinkage coefficients.

Experimental validation of the model

The objective of this validation was to observe how well the experimental results based on laboratory panels with various density profiles followed the prediction of the FE model. Each specific density profile represented was considered as a separate validation case and was simulated by the FE model. There were three laboratory MDF panels (replicates) per case. The density profiles of the sub-layer structures used for the simulations are given in Table 2. It can be seen for example that FE case no. 4 consists of 12 symmetrically distributed sub-layers, thinner in the surface layers.

Cases nos. 1, 2, and 3 represent panels with flat density profiles but with various average densities. This allows investigating the effect of panel average density (without the effect of density profile) on the level of warp. In fact, these three cases correspond to the three nominal density levels (540 kg/m³, 650 kg/m³, and 800 kg/m³) used to determine the physical and mechanical properties (Ganev et al. 2003, 2004a,

and 2004b) which serve as FE model parameters. The corresponding FE models consist in twelve layers with equal density.

Case no. 4 allows validating the model for a "regular" industrial–type panel, with a density profile characterized by high density (900 kg/m³) in the surface layers and low density (540 kg/m³) in the core layer. The corresponding FE model consists of two surface layers, each with two sub-layers of 900 kg/m³ and two sub-layers of 800 kg/m³, and a core layer with four sub-layers: two of 540 kg/m³ in the panel center and two of 650 kg/m³ adjacent to the surface layers.

Case no. 5 represents a panel with an asymmetrical density profile. Its core layer density is 650 kg/m³, and its surface layer density on the sealed panel side is 800 kg/m³. The opposite high-density surface layer is entirely omitted by sanding off. Case no. 5 allows the investigation of the effect of mistakes in the forming and pressing operations in MDF manufacturing. The corresponding FE model consists in one surface layer (with two sub-layers of 800 kg/m³ each) and a core layer (with ten sub-layers of 650 kg/m³ each).

All panels were initially conditioned to 50±2 % RH until equilibrium was reached. A silicone layer and a polyethylene foil were applied to one of the surfaces and to all panel edges. Forty-eight hours after application of the silicone, the

TABLE 2. *Density profiles of the experimental panels and distribution of the sub-layers in the corresponding FE models. The sealed surface is on the right.*

Case no.	Density profiles of experimental panels	Density of FE sub-layer (kg/m³)
1	540 kg/m³	540 540 540 540 540 540 540 540 540 540 540 540
2	650 kg/m³	650 650 650 650 650 650 650 650 650 650 650 650
3	800 kg/m³	800 800 800 800 800 800 800 800 800 800 800 800
4	900 kg/m³ / 540 kg/m³	900 900 800 800 650 540 540 650 800 800 900 900
5	800 kg/m³ / 650 kg/m³	650 650 650 650 650 650 650 650 650 650 800 800

level of warp of each panel was measured. The panels were immediately moved into a chamber maintained at 80 ± 2 % RH. The level of warp was monitored at 24-h intervals during the first week of exposure to 80 ± 2 % RH and then twice per week for the rest of the trials, which continued until equilibrium at 80 ± 2 % RH was reached (between 100 and 140 days). The monitoring of deformation in the x_3-direction at the cross-section of diagonals (Fig. 3) was conducted according to the NPA standard method for the measuring of warp (NPA 1996).

RESULTS AND DISCUSSION

A typical three-dimensional illustration of the warping calculated from the FE model is given in Fig. 4. An example of the transient moisture content profile is displayed in Fig. 5. The maximum and minimum levels of warp resulting from simulations and from the corresponding experiments are presented in Table 3.

Model validation

Symmetrical density profile.—Figure 6 presents the development of warp against time measured in the experimental trials and the results from the corresponding FE simulation for a MDF panel (Table 2, case no. 4) with a symmetrical density profile. It can be seen that both the experimental and the FE results show a maximum positive warp within 51 h of exposure to 80 % RH. The warp then gradually reduces to

reach the initial zero level after approximately 3000 h.

Asymmetrical density profile.—Figure 7 presents the experimental results and the corresponding FE simulation for case no. 5 from Table 2
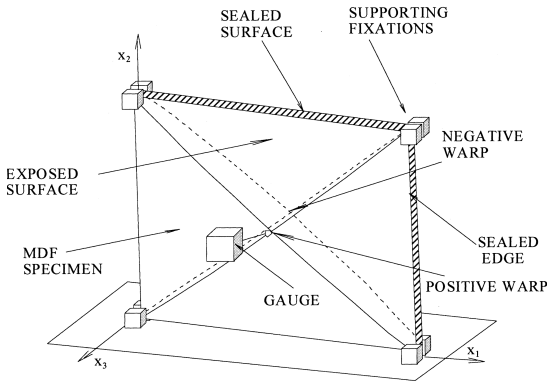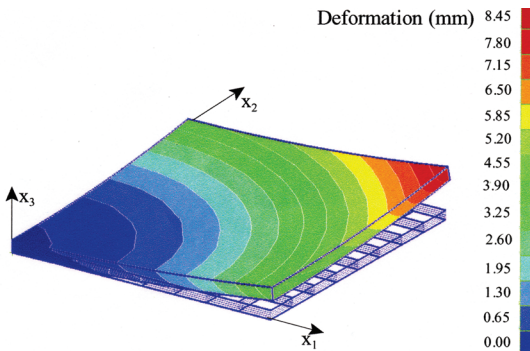

FIG. 3.   Setup for measuring warp.

FIG. 4.   Warping calculated from the FE model for case no. 4 after 51 h of adsorption from the exposed (bottom) surface. Model corresponds to one-fourth of the panel.
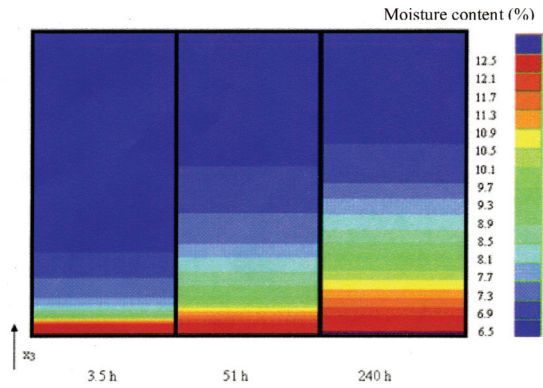

FIG. 5.   Moisture content profile across panel thickness (10.5 mm) after 3.5 h, 51 h, and 240 h of moisture adsorption from the exposed (bottom) surface.

(panel with density profile skewed towards the sealed surface). In this case, the experiment and the FE simulation lead to a negative final warp.

For the symmetrical and asymmetrical cases, the maximum levels of warp calculated by the FE model and the corresponding times differed from the experimental values by a maximum of 10 %. We attribute these small differences to the inevitable dissimilarities between the actual panels and the FE models: fluctuations in panel density profile and deviations of the actual panel properties from those used in the FE model (e.g. linear expansion coefficient as a function of density, or E_1 as a function of M and density).

The above differences of 10 % actually correspond to levels of warp inferior to 1 mm over a 792-mm span (the length of the diagonal at the panel surface) and are in the order of magnitude of the accuracy of the warp-monitoring method.

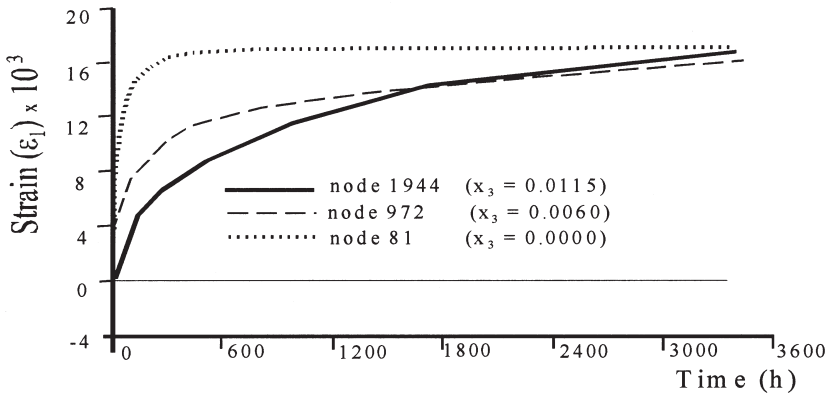TABLE 3.   *Maximum and minimum levels of warp and time to reach maximum warp.*

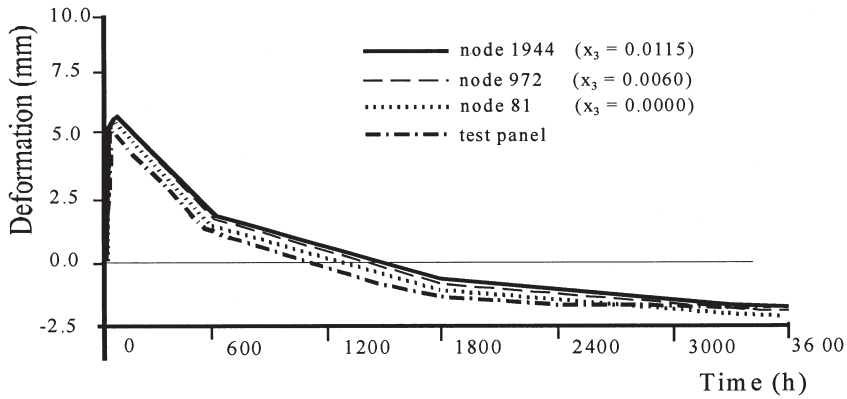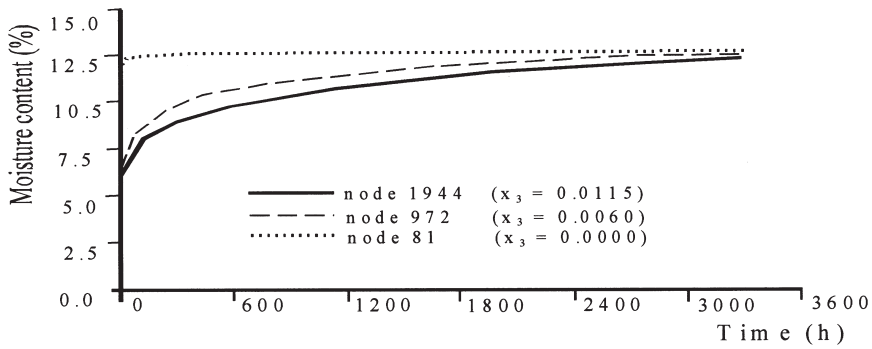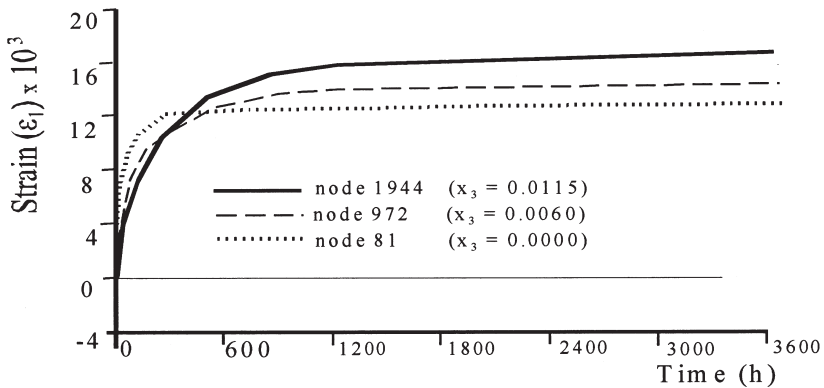|	Experimental data						FE model		
	Maximum		Time to max		Minimum			Time to	
	Mean	STD	Mean	STD	Mean	STD	Max	max	Min
Case no.	(mm)	(mm)	(h)	(h)	(mm)	(mm)	(mm)	(h)	(mm)
1	4.5	0.5	110	5.0	0.0	0.0	4.0	125	0.0
2	5.5	0.5	170	7.5	0.0	0.0	5.0	190	0.0
3	8.0	0.8	250	8.0	0.0	0.0	8.5	280	0.0
4	7.8	0.8	45	3.5	0.0	0.0	8.4	51	0.0
5	5.6	0.7	45	4.0	–2.0	0.0	5.5	53	–2.4

(a)

(b)

(c)

FIG. 6.   Experimental results and FE simulation for case no. 4 (standard case). (a) evaluation of warp; (b) moisture content evolution in the x_3 direction; (c) strain in the x_1 direction.

(a)

(b)

(c)

FIG. 7. Experimental results and FE simulation for case no. 5 (density profile skewed towards the sealed side). (a) evolution of warp; (b) moisture content evolution in the x_3 direction; (c) strain in the x_1 direction.

It is below the 15 % error specified by Lang et al. (1995) and it is negligible for the end-uses of the furniture and flooring industries. Therefore, we conclude that the model is valid and that the physical and mechanical properties determined in previous works (Ganev et al. 2004a, b) correctly characterize the laboratory MDF panels considered in this study.

Fundamentals of MDF panel warping

A schematic drawing of the stages of the warp process is presented in Fig. 8.

The results from the FE simulations show that panels with symmetrical density profiles (Table 2, cases no. 1, 2, 3, and 4) are flat at initial equilibrium to 50 % RH (which maintains M at approximately 6 %). This reflects the fact that the strains through panel thicknesses at initial M level are constant (Fig. 8, stage no. 1). When exposed to higher RH (e.g. 80 % RH), moisture starts penetrating through panel thickness. The exposed layers experience a maximum level of positive strain while the levels of strain of the layers closer to the sealed surface are lower, since their M has not changed yet (Fig. 8 stage no. 2 and Fig. 6 b and Fig. 6 c). As a consequence, an important strain differential through

panel thickness develops and the panel rapidly reaches a maximum warp corresponding to the maximum M-differential between the exposed layer and the sealed layer. With the progression of moisture diffusion through the panel, the level of warp gradually decreases, because the M-gradient and from there the strain gradient decrease. Finally, the panel returns to a flat shape when the strain equalizes throughout panel thickness (Fig. 8 stage no. 3 and Fig. 6 c).

The graphs obtained from the FE model (e.g. Fig. 6 a) show that at equilibrium at 80 % RH, a slight level of deformation remains in the x_3 direction. This is due to thickness swell induced by the M-increase. Stage 3 from Fig. 8, shows that the in-plane (x_1 and x_2) dimensions have also increased.

The negative final warp obtained in case no. 5 from Table 2 (Fig. 7 a) is explained by the fact that when moisture reaches the higher density layers, close to the sealed surface (Fig. 7 b), they expand more than the layers closer to the exposed surface (Fig. 10 c). As a result, the initially positive warp changes into negative.

The panel property that seems to have the strongest impact on warp is the LEC. Both the experimental results and the FE simulations showed a higher level of warp in the panels with higher average density without profile compared to pan-
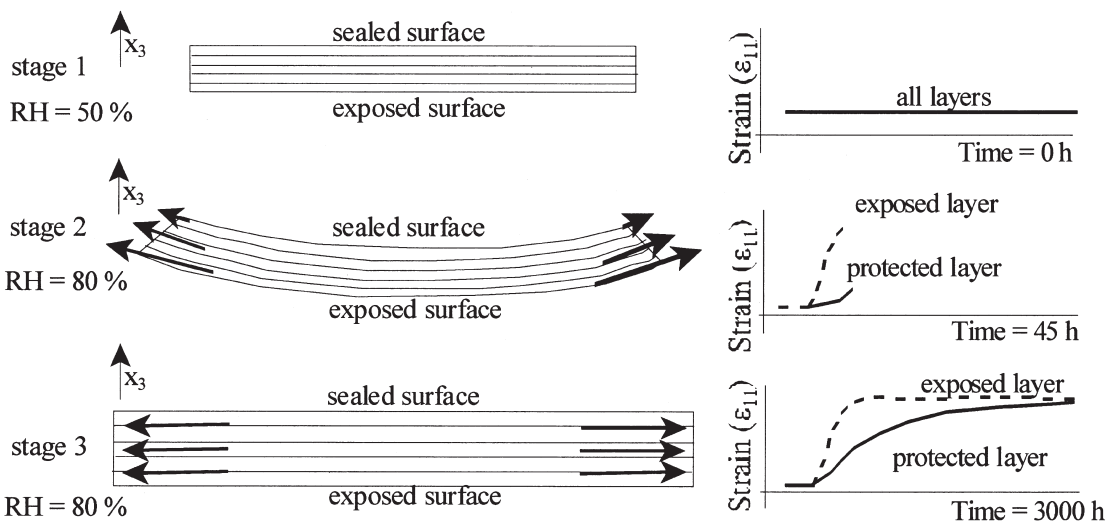

FIG. 8.   Stages in warp development (case no. 4 from Table 2). The arrows represent time variations of ϵ_1.

els with lower average density (e.g. Tab. 3, case no. 1, 2 and 3). The strong correlation between density and linear expansion coefficient (LEC) in MDF (Ganev et al. 2004b) results in higher strains in panels with higher average density and as a result to a higher maximum level of warp.

Panel density and density profile seem to have the strongest impact on warp since they affect all panel properties. A comparison among the results from cases no. 1, 2, and 3 (Tables 2 and 3) showed that the level of maximum warp increased, and it was attained later when the average density of panels with a flat density profile increased. The same effect was observed when the sharpness of the density profile increased. For example case no. 4 (with profile) has a higher maximum warp (Table 3) compared to case no. 2 (without profile, but with similar average density). This can be explained by the effect of density on the LEC and, as a result, on the expansion strain: the higher the density gradient, the higher the strain gradient and therefore, the higher the level of warp.

The warp that was observed in this study remained symmetrical in the panel plane. This confirmed our hypothesis of isotropy in the panel plane. The symmetry of the deformation in the panel plane demonstrates that the negative warp when observed was not a result of a saddle-shaped deformation, as described in the case of plywood by Suchsland et al. (1995). However, we feel that such an effect might be observed in MDF panels with strong fiber orientation.
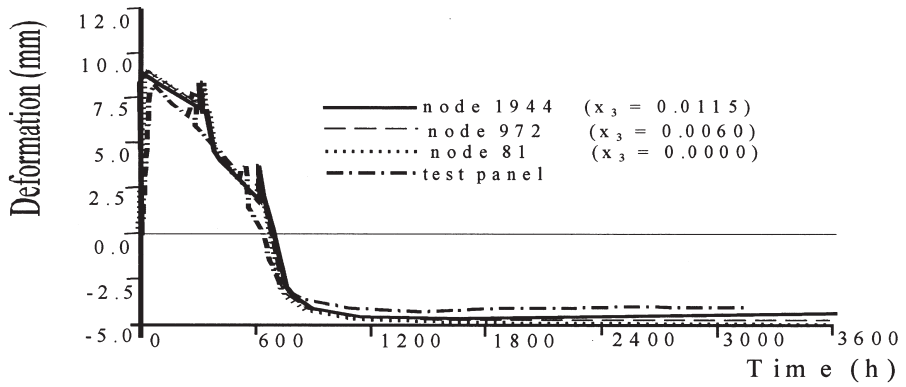
Special cases

Fluctuations in exposure relative humidity.—Relative humidity variation due to malfunction-ing of the conditioning chamber during the preliminary trials led to an unexpected warp development of test panels with a symmetrical density profile identical to case no. 4 from Table 2. Therefore, we decided to study this phenomenon in more detail. The results for this are presented in Table 4 (case no. 6). Figure 9 shows both experimental and FE results obtained following the RH fluctuations in the chamber. Exposed to a temporary RH increase (from 80 % RH to 86 % RH and then back to 80 % RH at two occasions, one of 24 h and another of 48 h), the panel instead of equilibrating to a flat form, went beyond the initial flatness position and continued deforming in the opposite direction, reaching a "negative" warp. Even though after the temporary fluctuation the RH returned to 80 % RH, the effect remained. The corresponding FE simulation led to a similar result (Table 4 and Fig. 9 a). A schematic representation of the phenomenon related to exposure to RH fluctuations is given in Fig. 10. We attribute this behavior of the MDF panels to the hysteresis between the adsorption and desorption branches of the relation between expansion coefficients and density as determined in previous work (Ganev et al. 2004b). Stages no. 1 and no. 2 are identical to the "standard" case as in Fig. 8. The difference is in the next stages no. 3 and no. 4. The initially flat panel (stage no. 1) when exposed to higher RH becomes convex towards the exposed surface (stage no. 2). Should the RH temporary increase (e.g. to 86 % RH for 24 h), additional moisture penetrates mainly into the exposed surface of the panel. This leads to an added positive strain (ϵ_1 and ϵ_2 or LEC) of the exposed surface layer, leading to a stronger convex (positive) warp (Fig. 10 stage no. 3 and Fig. 9 b and c). Following the return of RH to the nominal
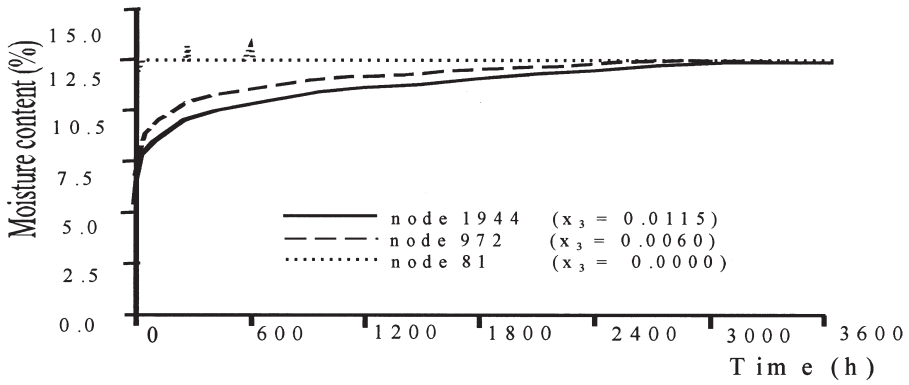
TABLE 4. *Maximum and minimum levels of warp and time to reach maximum warp for the special cases.*

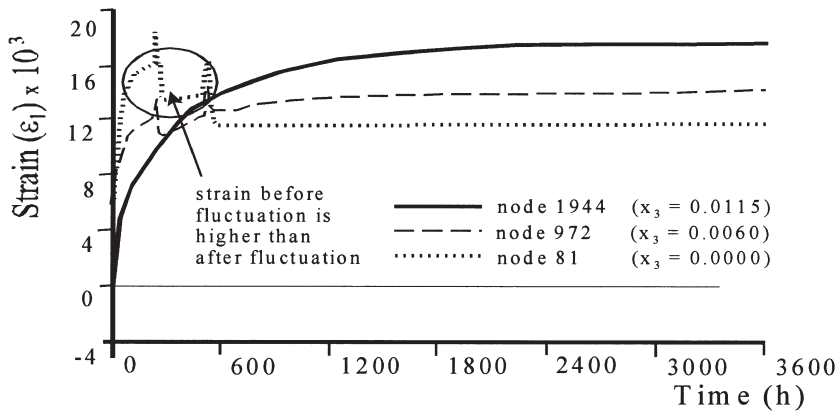|	Experimental data						FE model		
	Maximum		Time to max		Minimum			Time to	
	Mean	STD	Mean	STD	Mean	STD	Max	max	Min
Case no.	(mm)	(mm)	(h)	(h)	(mm)	(mm)	(mm)	(h)	(mm)
6	7.5	0.6	45	4.0	−3.5	0.0	8.4	53	−4.8
7			not available*				7.0	78	3.0
8			not available*				8.4	53	−5.2

* No experimental data available to validate the results from the FE model.

(a)

(b)

(c)

FIG. 9.   Experimental results and FE simulation for case no. 4 exhibiting RH-fluctuation. (a) evolution of warp; (b) moisture content evolution in the x_3 direction; (c) strain in the x_1 direction.

level (80 %), the exposed surface layer dries out to approximately the level of stage no. 2 experiencing a negative strain (ϵ_1 and ϵ_2 or LCC). Given the expansion hysteresis (LCC being usually much higher than LEC), the surface layer becomes shorter compared to stage no. 2. Depending on the level and amplitude of the temporary RH increases, warp changes from convex to concave towards the exposed surface (Fig. 10 stage no. 3 and Fig. 9c).

Simulations without experimental validation.—Two cases considered of interest were simulated with the FE model, and the results from simulations are presented in Table 4 for completeness, although experiments to validate the FE results were not performed. Given the validity of the model, it was assumed that the FE results still should be indicative.

Based on a FE simulation, a panel with a density profile skewed towards the exposed surface (a mirror image of case no. 5, Table 2) retains some level of positive warp at equilibrium to 80

% RH and does not reach the initial state of flatness (case no. 7 from Table 4). The FE simulation shows that in such panel, the positive strains (ϵ_1 and ϵ_2) of the exposed surface layers strongly exceed the strains of the balancing layers from the sealed side

A temporary decrease in chamber RH from 80 % RH to 74 % RH (Table 4 case no. 8) has a final effect similar to that describing a temporary RH increase. In the case of RH decrease, the strain in the surface reduces and has a permanent effect leading to negative (concave) warp.

CONCLUSIONS

The purpose of this study was to develop and validate a finite element model for simulation of the hygromechanical warping of MDF. The closeness of the experimental and FE results suggests that the elastic model adequately reflects the hygromechanical deformations in MDF at ambient temperature and could be used
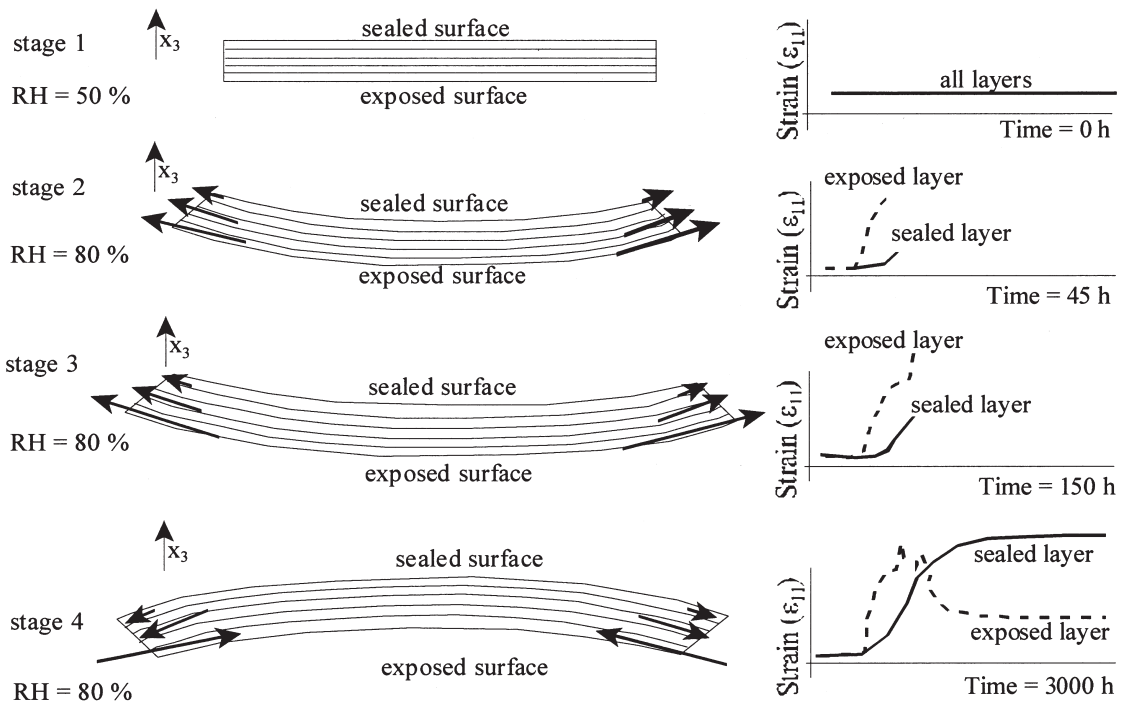

FIG. 10.   Stages in warp development as a function of RH fluctuation (case no. 4 from Tab. 2). The arrows represent time variations of ϵ_1.

for simulations of warp in industrial conditions and for design optimization of the MDF density profile.

Simulations with the finite element method and experimental results showed that the moisture content increase in the zones close to the surface at the early exposure stages causes rapidly a convex deformation towards the exposed surface. When moisture content gradually becomes homogenous across panel thickness, the panel returns to a flat shape. There is a strong effect of panel density profile on the levels of warp and its dynamics. For panels with a flat density profile, the higher the average panel density, the higher the level of warp due to the effect of density on the expansion properties. The panels presenting a sharper density profile experience higher strain differentials and therefore develop stronger warp compared to panels with a more even density profile. When the density profile is skewed towards the sealed surface, the panel continues to deform and develops a negative warp instead of stabilizing back to a flat form. Increase in exposure relative humidity may lead to changes of the warp from positive to negative due to the hysteresis in the linear expansion coefficient in adsorption and desorption. Symmetry of the deformation (along the x_1 and the x_2 edges) in the panel plane confirmed the concept of plane isotropy in the laboratory MDF panels. Simulations with the finite element model without experimental validation suggest that at constant exposure conditions when a density profile is skewed towards the exposed surface, the panel may not return to a flat form after developing positive warp. A decrease in exposure relative humidity may lead to change of the warp from positive to negative.

REFERENCES

BODIG, J., AND B.A. JAYNE. 1993. Mechanics of wood and wood composites. Van Nostrand Reinhold Company, New York, NY. 712 pp.

BOLTON, A. J., AND P.E. HUMPHREY. 1994.The permeability of wood-based composite materials. Part 1. A review of the literature and some unpublished work. Holzforschung 48: 95–100.

CLOUTIER, A., G. GENDRON, P. BLANCHET, S.B. GANEV, AND R. BEAUREGARD. 2001. Finite element Modeling of Dimensional Stability in Layered Wood Composites. 35th International Particleboard/Composite Materials Symposium, April 3- 5. Washington State University, Pullman, WA. 18 pp.

COMPOSITE PANEL ASSOCIATION (CPA). 1998. MDF from start to finish. Composite Panel Association, Gaithersburg, MD.

DENISOV, O.B., P.P. ANISOV, AND P.E. ZUBAN. 1975. Investigations on the permeability of particle mats. Holztechnologie 16 (1):10–14. In German with summary in English.

FOREST PRODUCTS LABORATORY. 1987. Wood handbook (Agriculture Handbook). Forest Service, U.S. Agriculture Department, Washington DC.

GANEV, S.B., AND A. CLOUTIER. 2002. Effect of average panel density and density profile on the linear expansion of particleboard and medium density fiberboard. Report submitted to the Composite Panel Association. Gaithersburg, MD.

———, ———, R. BEAUREGARD, AND G. GENDRON. 2003. Effect of moisture content and density on moisture movement in MDF panels. Wood Fiber Sci. 35(1): 68–82.

———, ———, G. GENDRON, AND R. BEAUREGARD. 2004a. Mechanical properties of MDF as a function of density and moisture content. Wood Fiber Sci. (submitted).

———, ———, BEAUREGARD, AND G. GENDRON. 2004b. Linear expansion and thickness swell of MDF as a function of panel density and sorption branch. Wood Fiber Sci. (submitted).

HEEBINK, B.G., E. W. KUENZI, AND A.C. MAKI. 1964. Linear movement of plywood and flakeboards as related to the longitudinal movement of wood. Forest Products Laboratory, Madison, WI.

ISMAR, H., AND M. PAULITSCH. 1995. Effect of climate on the residual stresses and deformations of multi-layered particle boards. Holz Roh-Werkst. 53:369–376.

KEYLWERTH, R. 1958. The mechanics of multilayer particle boards Holz Roh- Werkst. 16(11):419–430.. In German with sumary in English.

LANG, E.M., J.R. LOFERSKI AND J.D. DOLAN. 1995. Hygroscopic deformation of wood-based composite panels Forest Prod.J. 45(3):67–70.

NATIONAL PARTICLEBOARD ASSOCIATION (NPA). 1996. Standard method for measuring of warp in particleboard and medium density fiberboard (MDF). NPA 18928 premiere Court, Gaithersburg, MD.

PLATH, E. 1972. Calculations [relating to the design] of wood-based sandwich materials. Holz Roh- Werkst. 30 (2):57–61.

SCHNEIDER, A., E. ROFFAEL AND H.A. MAY. 1982. Investigations on the influence of density, resin level and flake dimensions on the sorption behaviour and thickness swelling of particleboards. In German with summery in English. Holz Roh- Werkst. 40:339–344.

SIAU, J.F. 1995. Wood: Influence of moisture to its physical properties. Department of Wood Science and Forest Products, Virginia Polytechnic Institute and State University, Blacksburg, VA. 227 pp.

SUCHSLAND, O. 1973. Hygroscopic Thickness swelling and related properties of selected commercial particleboards. Forest Prod. J. 23 (7): 26–30.

———, AND J. D. MCNATT. 1985. On the warping of laminated wood products. Michigan State University, East Lansing, MI.

———, AND ———. 1986.Computer simulation of laminated wood panel warping. Forest Prod. J. 36(11–12): 16–23.

———, Y. G. FENG, AND D.P. XU. 1995. The hygroscopic warping of laminated panels Forest Prod. J. 45(10): 57–63.

TONG, Y., AND O. SUCHSLAND. 1993. Application of finite element analysis to panel warping Holz- Roh- Werkst., 51(1): 55–57.

VITAL, B.R., AND J. B.WILSON. 1979. Factors affecting the water adsorption of particleboard and flakeboard.Symposium on wood moisture content - temperature and humidity relationships, Virginia Polytechnic Institute and State University, Blacksburg, VA, Oct. 29, 1979, 97–101; Forest Products Laboratory, USDA Forest Service, Madison, WI.

WINISTORFER, P.M, AND W. XU. 1996. Layer water absorption of medium density fiberboard and oriented strandboard Forest Prod. J. 46(6):69–72.

WOODSON, G.E. 1975. Effects of bark, density profile, and resin content on medium-density fiberboards from southern hardwoods. Forest Prod. J. 26 (2) : 39–43.

XU, H. 1993. Application of a linear viscoelastic plate theory to hygroscopic warping of laminates. A dissertation submitted Michigan State University. East Lansing, MI.

XU, D. 1994. Theoretical and experimental investigation on hygroscopic warping of wood composite panels. A dissertation submitted to Michigan State University. East Lansing, MI.

———, XU D., AND O. SUCHSLAND. 1996. A modified elastic approach to the theoretical determination of the hygroscopic warping of laminated wood panels, Wood Fiber Sci., 28(2):194–204.

XU, W., P.M. WINISTORFER, AND W.W. MOSHLER. 1996. A procedure to determine water absorption distribution in wood composite panels. Wood Fiber Sci., 28(3): 286–294.